Heat-Shock and Redox-Dependent Functional Switching of an h-Type Arabidopsis Thioredoxin from a Disulfide Reductase to a Molecular Chaperone[1[C][W][OA]]

Soo Kwon Park[2], Young Jun Jung[2], Jung Ro Lee[2], Young Mee Lee, Ho Hee Jang, Seung Sik Lee, Jin Ho Park, Sun Young Kim, Jeong Chan Moon, Sun Yong Lee, Ho Byoung Chae, Mi Rim Shin, Ji Hyun Jung, Min Gab Kim, Woe Yeon Kim, Dae-Jin Yun, Kyun Oh Lee, and Sang Yeol Lee*

Environmental Biotechnology National Core Research Center, Plant Molecular Biology and Biotechnology Research Center (S.K.P., Y.J.J., J.R.L., Y.M.L., H.H.J., S.S.L., J.H.P., S.Y.K., J.C.M., S.Y.L., H.B.C., M.R.S., J.H.J., W.Y.K., D.-J.Y., K.O.L., S.Y.L.), and Division of Applied Life Science (BK21 program; S.K.P., Y.J.J., J.R.L., Y.M.L., S.S.L., J.H.P., S.Y.K., J.C.M., S.Y.L., H.B.C., M.R.S., J.H.J., D.-J.Y., K.O.L., S.Y.L.), Gyeongsang National University, Jinju 660–701, Korea; Lee Gil Ya Cancer and Diabetes Institute, Gachon University of Medicine and Science, Incheon 406–840, Korea (H.H.J.); Department of Functional Crop, National Institute of Crop Science, Rural Development Administration, Milyang 627–130, Korea (S.K.P.); and Bio-crops Development Division, National Academy of Agricultural Science, Rural Development Administration, 224 Suin-ro, Suwon 441–857, Korea (M.G.K.)

A large number of thioredoxins (Trxs), small redox proteins, have been identified from all living organisms. However, many of the physiological roles played by these proteins remain to be elucidated. We isolated a high M_r (HMW) form of h-type Trx from the heat-treated cytosolic extracts of Arabidopsis (*Arabidopsis thaliana*) suspension cells and designated it as AtTrx-h3. Using bacterially expressed recombinant AtTrx-h3, we find that it forms various protein structures ranging from low and oligomeric protein species to HMW complexes. And the AtTrx-h3 performs dual functions, acting as a disulfide reductase and as a molecular chaperone, which are closely associated with its molecular structures. The disulfide reductase function is observed predominantly in the low M_r forms, whereas the chaperone function predominates in the HMW complexes. The multimeric structures of AtTrx-h3 are regulated not only by heat shock but also by redox status. Two active cysteine residues in AtTrx-h3 are required for disulfide reductase activity, but not for chaperone function. AtTrx-h3 confers enhanced heat-shock tolerance in Arabidopsis, primarily through its chaperone function.

Thioredoxin (Trx) is a ubiquitous multifunctional redox protein with a single disulfide bridge. It functions as a general disulfide oxidoreductase and is involved in numerous redox-dependent cellular processes including activation of ribonucleotide reductase, modulation of transcription factors, promotion of a variety of tumors, and photosynthetic activity of plant cells (Aslund and Beckwith, 1999; Balmer et al., 2003; Ravi et al., 2005). Trxs also control several redox-independent cellular reactions, such as assembly of the T7 DNA polymerase complex and the formation of filamentous phage (Feng et al., 1997; Hamdan et al., 2005), whose reaction mechanisms have yet to be elucidated.

The complexity of Trx systems in plants is distinctive compared with nonphotosynthetic organisms. In the fully sequenced Arabidopsis (*Arabidopsis thaliana*) genome (The Arabidopsis Genome Initiative, 2000), at least six major groups of Trxs have been identified, including Trx-m, -f, -x, -y, -o, and -h. The Trx-m, -f, -x, and -y proteins are located in the chloroplasts and regulate the redox status of enzymes involved in photosynthesis and light-dependent CO_2 fixation (Wolosiuk et al., 1993). Trx-o proteins are distributed in the mitochondria (Laloi et al., 2001). Trx-h proteins are typically localized in the cytoplasm, but they have also been identified in other cellular compartments such as the mitochondria, endoplasmic reticulum (Marcus et al., 1991; Ishiwatari et al., 1995), and even the nucleus (Serrato and Cejudo, 2003). However, only a few functions have been elucidated for the h-type Trxs, which represent the largest group of these proteins identified by sequencing (Laloi et al., 2004).

[1] This work was supported by a MOEST/KOSEF for the EB-NCRC (grant no. R15–2003–012–01001–0), WCU program (grant no. R32–10148), and NRL (grant no. M10600000205–06J0000–20510). Scholarship of the first four authors was supported by the BK21 program, Korea.

[2] These authors contributed equally to the article.

* Corresponding author; e-mail sylee@gnu.ac.kr.

The author responsible for the distribution of materials integral to the findings presented in this article in accordance with the policy described in the Instructions for Authors (www.plantphysiol.org) is: Sang Yeol Lee (sylee@gnu.ac.kr).

[C] Some figures in this article are displayed in color online but in black and white in the print edition.

[W] The online version of this article contains Web-only data.

[OA] Open access articles can be viewed online without a subscription.

www.plantphysiol.org/cgi/doi/10.1104/pp.109.135426

Although Trxs exhibit distinctive biochemical properties, they all demonstrate high levels of amino acid sequence similarity and contain a common structural motif, the Trx-fold. This motif comprises approximately 80 amino acid residues, with a central core of five β-strands enclosed by four α-helices and two hydrophobic zones (Katti et al., 1990). Some proteins harboring the Trx-fold have also been shown to function as molecular chaperones. These include protein disulfide isomerase (PDI) and 2-Cys peroxiredoxins (Prxs; Quan et al., 1995; Jang et al., 2004). It is presumed that the Trx-fold-containing proteins interact with other proteins at the hydrophobic surface around their active site.

Considering the fact that 2-Cys Prxs reversibly changed their protein structures from low M_r (LMW) to high M_r (HMW) complexes by heat shock concomitantly with functional changes from a peroxidase to a molecular chaperone (Jang et al., 2004; Chuang et al., 2006), we decided to screen heat-shock-induced HMW proteins that share a similar regulation mode with the 2-Cys Prxs from heat-treated Arabidopsis suspension cells. Using size exclusion chromatography (SEC) and matrix-assisted laser desorption ionization time-of-flight (MALDI-TOF) techniques, a highly heat-stable h3-isoform of Arabidopsis Trx having a HMW structure was isolated and designated AtTrx-h3 (GenBank accession no. At5g42980). Given that the Trxs can interact with a number of proteins (Marchand et al., 2004) and that *Escherichia coli* Trx displays the refolding activity of molecular chaperone (Kern et al., 2003), in this study, we investigated the chaperone function and structural changes of AtTrx-h3 by in vitro experiments and the functional roles of the protein by in vivo tests.

RESULTS

Subcellular Localization of AtTrx-h3 in Arabidopsis

To analyze the physiological function of heat-stable AtTrx-h3 in plants, we first used a fluorescence microscope to analyze the subcellular localization of AtTrx-h3 tagged with GFP at its C terminus. When the AtTrx-h3-GFP DNA construct was transformed into Arabidopsis protoplasts, the fluorescence was distributed throughout the cytoplasm (Fig. 1A) and typically overlapped with that of an authentic cytosolic protein, malate dehydrogenase (MDH; Fig. 1B), which was tagged with red fluorescent protein (RFP; Fig. 1D). Also, when we merged the green fluorescence of AtTrx-h3 with the autofluorescence signal of chloroplasts (Fig. 1C), the green fluorescence was clearly distinguished from the chloroplast autofluorescence (Fig. 1E). From these results, we concluded that AtTrx-h3 is localized to the plant cytoplasm.

AtTrx-h3 Plays Dual Functions, Acting as a Disulfide Reductase and as a Molecular Chaperone

It has been shown that the disulfide reductase function is a peculiar characteristic of Trx proteins. Therefore, after purifying the bacterially expressed recombinant AtTrx-h3 protein to homogeneity (Supplemental Fig. S1), we measured the ability of AtTrx-h3 to reduce 5,5′-dithio-*bis*(2-nitrobenzoic acid) (DTNB) in the presence of NADPH and Trx reductase as reductants and observed that DTNB reduction increased linearly with increasing AtTrx-h3 concentrations (Fig. 2A; Holmgren and Bjornstedt, 1995). However, when we assessed the disulfide reduction activity by using insulin as a substrate in the presence of 0.5 mM dithiothreitol (DTT), AtTrx-h3 clearly exhibited reduction activity at lower concentrations (3 or 5 μM; Fig. 2B). Surprisingly, however, at concentrations above 10 μM, the insulin reduction activity dropped significantly with increasing AtTrx-h3 concentration. The results presented in Figure 2B strongly suggests that at higher molar ratios of AtTrx-h3 to protein substrate, the reduced and partially denatured insulin produced by its disulfide reductase activity is instantaneously trapped by AtTrx-h3 in soluble complexes, which is a

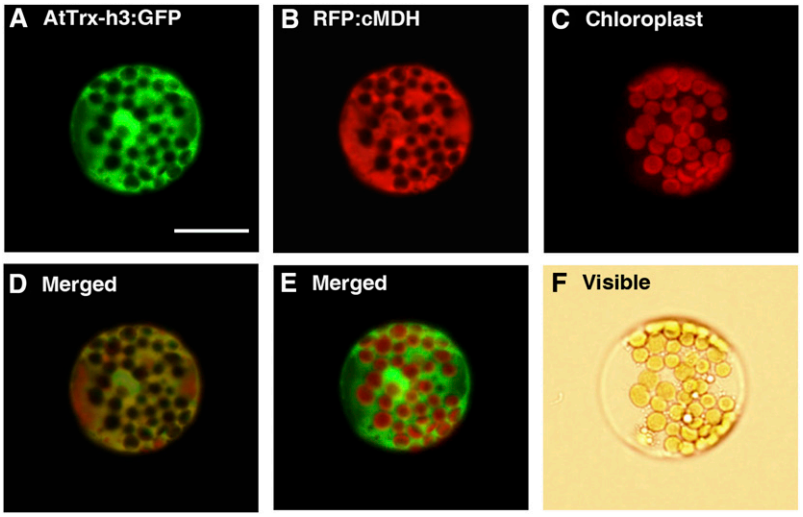

Figure 1. Subcellular localization of AtTrx-h3 in Arabidopsis protoplast cells. Protoplasts isolated from 10-d-old Arabidopsis were transformed with AtTrx-h3-GFP and a standard cytosolic type of MDH fused with RFP (RFP-cMDH) DNAs, respectively. GFP fluorescence (A), RFP fluorescence (B), and chloroplast autofluorescence (C) were observed under a fluorescence microscope. The fluorescence image of GFP precisely overlapped with that of RFP as shown by the yellow colors (D), but not with the autofluorescence of chloroplasts (E). Visible images of cell morphology (F) were taken under bright-field microscopy. Scale bar, 20 μm.

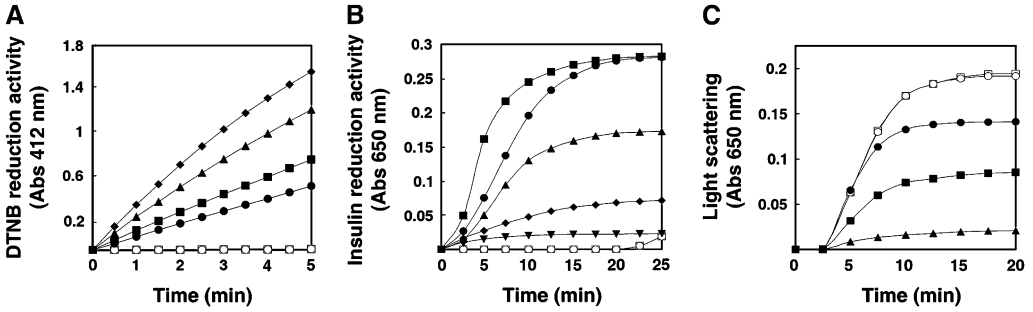

Figure 2. Dual functions of AtTrx-h3 acting as a disulfide reductase and as a molecular chaperone. A and B, Disulfide reduction activity of AtTrx-h3. A, Reduction of DTNB (5 mM) disulfide bonds was measured in the presence of NADPH and Trx reductase at the presence of 3 mM (●), 5 mM (■), 10 mM (▲), and 20 mM (♦) AtTrx-h3. B, Reduction of insulin (30 mM) disulfide bonds was assayed in the presence of 0.5 mM DTT at the concentrations of 3 mM (●), 5 mM (■), 10 mM (▲), 20 mM (♦), and 30 mM (▼) AtTrx-h3. C, Chaperone activity of AtTrx-h3. Thermal aggregation of 1 mM MDH was examined at 45°C for 20 min in the presence of AtTrx-h3. Molar ratios of AtTrx-h3 to MDH measured were at 1:1 (●), 3:1 (■), and 6:1 (▲). Reactions (A–C) measured with 30 mM ovalbumin (○) instead of AtTrx-h3 or lacking both AtTrx-h3 and ovalbumin (□) were used as controls. Abs, Absorbance.

property typical of molecular chaperone (Datta and Rao, 1999).

To test this assumption, we examined the chaperone function of AtTrx-h3 by assessing its ability to inhibit the thermal aggregation of a substrate, MDH. Incubation of MDH with increasing amounts of AtTrx-h3 gradually prevented thermal aggregation of the substrate, which could be significantly blocked at a subunit molar ratio of 1 MDH to 6 AtTrx-h3 (Fig. 2C). In addition, when we assayed the chaperone function of AtTrx-h3 with the use of citrate synthase (CS) or luciferase as substrates, similar results were obtained (Supplemental Fig. S2), suggesting that AtTrx-h3 protects a wide range of protein substrates from denaturation. In contrast, when we replaced AtTrx-h3 with 30 μM ovalbumin in the reaction mixture as a control,

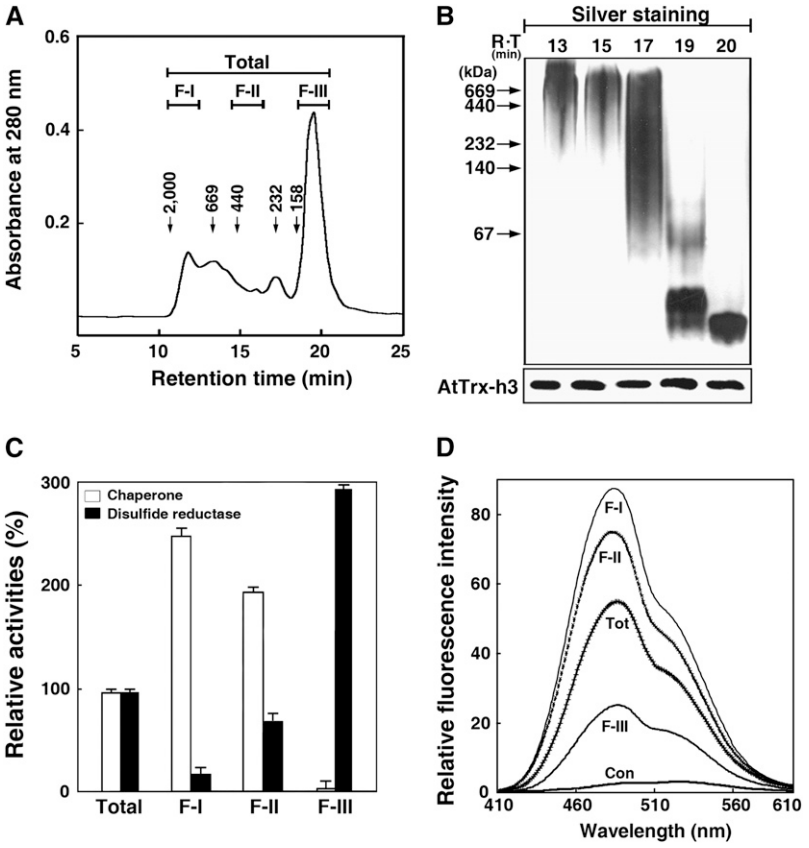

Figure 3. AtTrx-h3 functions are associated with its differently sized multiple protein structures. A, AtTrx-h3 fractions separated by SEC with a TSK G4000SWx_L column were pooled as indicated by the bars on the chromatogram (F-I, F-II, and F-III) for further analysis. B, Each fraction in the SEC was subjected to silver staining following separation on 10% native PAGE (top section) and 12% SDS-PAGE (bottom section) gels. The numbers in A (arrows on the chromatogram) and B (on the left side) represent the MWs of protein standards. C, After equalizing the AtTrx-h3 levels in the three SEC fractions (F-I to approximately F-III in A) and in an aliquot of total protein, their specific chaperone activities with MDH as a substrate (white bar), and disulfide reduction activities with DTNB as a substrate (black bar) were measured. Activities in the different protein fractions were compared with those of total protein. The total protein activities were measured at A_{412} (DTNB reduction activity) and A_{650} (chaperone activity) after 5 and 20 min reaction under our assay conditions and set to 100%, respectively. D, Comparison of hydrophobicity between the SEC-separated fractions. Bis-ANS (10 μM) was incubated with AtTrx-h3 (2 μM) proteins separated from SEC, such as total (Tot), F-I, F-II, F-III, and without protein (Con), at 25°C for 30 min. Fluorescence intensities of bis-ANS were measured using an excitation wavelength of 390 nm and emission wavelengths from 400 to 600 nm.

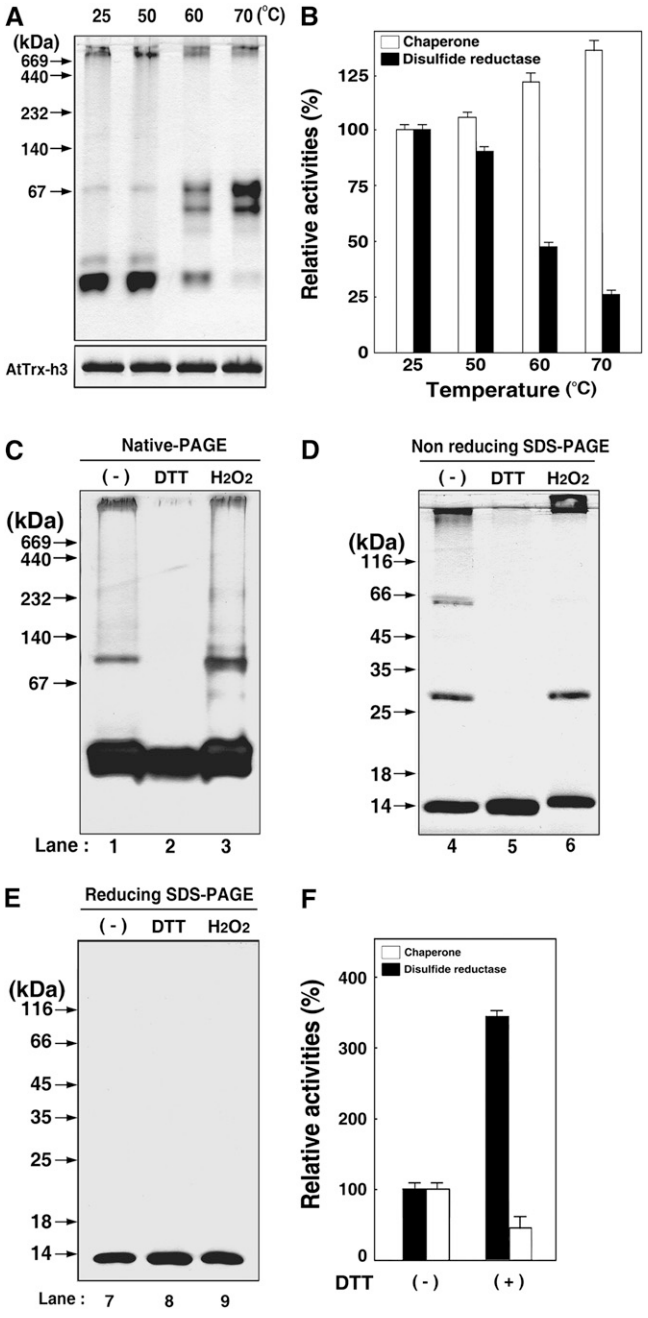

Figure 4. Heat-shock and redox-dependent structural changes of AtTrx-h3 in vitro. A, Structural changes of AtTrx-h3 incubated at various temperatures for 30 min were analyzed by silver staining of 10% native PAGE (top section) or 12% SDS-PAGE (bottom section) gels. B, Relative activities of DTNB reduction (black bar) and chaperone (white bar) functions of heat-treated AtTrx-h3 were compared with those of native AtTrx-h3 incubated at 25°C. The activities of native AtTrx-h3 were measured at A_{412} (DTNB reduction activity) and A_{650} (chaperone activity) after 5 and 20 min reaction under our assay conditions and set to 100%, respectively. C to E, Redox-dependent structural changes of AtTrx-h3 were analyzed by silver staining on 10% native PAGE (C), 12% nonreducing SDS-PAGE (D), and reducing SDS-PAGE (E) gels. Purified AtTrx-h3 (lanes 1, 4, 7), 20 mM DTT-treated AtTrx-h3 (lanes 2, 5, 8), and 20 mM H_2O_2-treated AtTrx-h3 after removal of DTT (lanes 3, 6, 9) were loaded to the PAGE gels, respectively. F, Redox-dependent activity changes of AtTrx-h3. DTNB reduction (black bar) and chaperone (white bar) activities of AtTrx-h3 measured in the presence of 20 mM DTT were compared with the activities measured in the absence of DTT, which were set to 100%. The activities were checked at A_{412} (DTNB reduction activity) and A_{650} (chaperone activity) after 5 and 20 min reaction under our assay conditions, respectively.

neither the disulfide reductase nor chaperone activities were detected, suggesting that the dual activities were derived from the specific function of AtTrx-h3.

AtTrx-h3 Produces Various Forms of HMW Protein Complexes That Are Specifically Associated with Different Activities

In general, most chaperone proteins associate into dimers, trimers, and higher oligomeric complexes (Haley et al., 1998). Since AtTrx-h3 exhibits a chaperone function (Fig. 2C), we investigated the molecular sizes of the purified recombinant AtTrx-h3 by SEC and identified a variety of different protein complexes (Fig. 3A). The various sizes of AtTrx-h3 protein structure in each fraction were confirmed by silver staining on a 10% native PAGE gel (Fig. 3B, top section). The molecular sizes of the proteins in the first SEC fraction, which contained the largest AtTrx-h3 complexes, were too high to penetrate the pores of a 10% native PAGE gel, but the sizes of the other fractions of the SEC ranged from approximately 10 to 1,000 kD. In contrast, all the protein fractions of AtTrx-h3 produced a single protein band on a SDS-PAGE gel, and the estimated MW of the monomeric subunit was 13.1 kD (Fig. 3B, bottom section). These results suggest that the multiple peaks observed by SEC of AtTrx-h3 are composed of homopolymeric protein structures.

As AtTrx-h3 formed various multimeric protein structures and demonstrated dual activities, we investigated the specific activities of the three protein fractions separated by SEC (F-I to F-III in Fig. 3A). To test whether the protein structures of each fraction were stable, the protein fractions were subjected to rechromatography under the same conditions described in Figure 3A. We found that the protein structures of each fraction were stable enough to characterize their biochemical properties in vitro (Supplemental Fig. S3). In contrast to the LMW protein fraction (F-III), the proteins in the F-I and F-II fractions exhibited a strong chaperone activity (Fig. 3C). However, proteins in the F-III fraction demonstrated a strong disulfide reduction activity, with no chaperone function. To analyze the differences in chaperone activity between the AtTrx-h3 fractions, we compared the hydrophobicity of the proteins using the fluorescent compound 1,1′-bi (4-anilino) naphthalene-5,5′-disulfonic acid (bis-ANS), which binds hydrophobic regions (Sharma et al., 1998). We found that the fluorescence intensity of protein-bound bis-ANS was greatest for fraction F-I, less for fractions F-II, Tot, and F-III, and was negligible for the protein-free control (Fig. 3D). These data sug-

gest that the chaperone activity of the complexes is in direct proportion to their degree of hydrophobicity. Thus, the chaperone function of AtTrx-h3 occurs predominantly in the HMW complexes, whereas the disulfide reduction activity occurs in the LMW species.

Effect of Heat-Shock and Redox Status on the Protein Structure and Function of AtTrx-h3 in Vitro

We analyzed the effect of heat shock on the AtTrx-h3 structures using a native PAGE gel and found that the protein structures of AtTrx-h3 were changed in vitro by incubating the protein above 50°C (Fig. 4A). As the temperature increased, the oligomeric protein peaks increased concomitantly with a decrease in the levels of LMW proteins. In addition to the structural changes, the chaperone activity of AtTrx-h3 increased following heat shock, whereas the DTNB reduction activity of AtTrx-h3 rapidly decreased with the heat treatment (Fig. 4B).

As oxidative stress was reported to play a major role in the detrimental effect of heat shock in eukaryotes (Davidson et al., 1996) and reducing conditions are a prerequisite for measuring disulfide reduction activity, we analyzed the redox-dependent structural changes of AtTrx-h3 under various conditions of PAGE. Purified AtTrx-h3 displayed multimeric protein structures in native PAGE conditions (Fig. 4C, lane 1). However, reduction of AtTrx-h3 by DTT prior to native PAGE changed the structures into LMW protein species (lane 2). Also, subsequent treatment of hydrogen peroxide (H_2O_2) after removal of DTT almost restored the protein structures of AtTrx-h3 (lane 3), suggesting that the structural changes of AtTrx-h3 are dependent on redox status, which was confirmed by SEC (Supplemental Fig. S4). Also, in the presence of an excessive amount of SDS detergent (1%) in nonreducing SDS-PAGE conditions, AtTrx-h3 still produced SDS-resistant polymeric structures (Fig. 4D, lane 4), indicating that the major force of their oligomerization should be the hydrophobic interactions. However, when AtTrx-h3 was incubated with DTT prior to nonreducing SDS-PAGE, the multimeric structures of AtTrx-h3 were completed dissociated into monomers (lane 5). The DTT-induced monomerization of AtTrx-h3 in a nonreducing SDS-PAGE gel was restored to the original structures by treatment with H_2O_2 for 1 h (lane 6). In contrast, H_2O_2 failed to oligomerize AtTrx-h3 in the presence of a reducing agent, such as DTT or β-mercaptoethanol, during reducing SDS-PAGE (Fig. 4E, lanes 7–9). These observations suggest that AtTrx-h3 polymeric structures are associated not only by the forces of hydrophobic interactions, but also by redox-dependent disulfide bonds. Accompanying with the redox-dependent structural changes, the dual functions of AtTrx-h3 are also switched by the redox changes. The treatment of DTT induces a significant increase of the DTNB reduction activity but critically decreases the chaperone activity of AtTrx-h3 (Fig. 4F).

Based on the results of the redox-dependent structural changes of AtTrx-h3, we investigated the role of the two highly conserved Cys residues in AtTrx-h3 protein structure and function. For this purpose, we

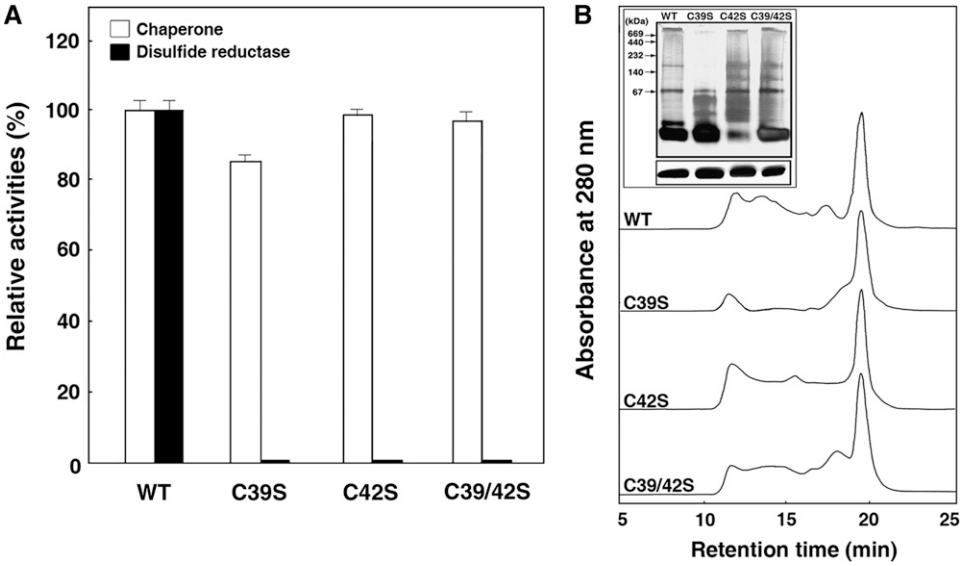

Figure 5. Effect of Cys residues on the dual functions of AtTrx-h3 and its protein structures. A, Comparison of the disulfide reductase and chaperone activities between the native form of AtTrx-h3 and mutant proteins containing site-specific replacement of two conserved Cys residues by Ser (C39S, C42S, and C39/42S). Activities of mutant proteins were compared with those of native AtTrx-h3. The native AtTrx-h3 activities were measured at A_{412} (DTNB reduction activity) and A_{650} (chaperone activity) after 5 and 20 min reaction under our assay conditions and set to 100%, respectively. B, Structural changes of the Cys-mutant proteins were analyzed by SEC, native PAGE, and SDS-PAGE (inset), followed by silver staining. WT, Wild type.

prepared recombinant proteins in which one or both of the Cys residues were replaced by Ser residues (C39S, C42S, and C39/42S) and assayed the functions of the mutant proteins. Although the two Cys residues of AtTrx-h3 were essential for disulfide reduction activity, the chaperone activity of the mutant proteins was almost the same as that of native AtTrx-h3 (Fig. 5A). In accordance with this, there was only a little difference between the HMW protein peaks of native AtTrx-h3 and those of the Cys mutants in SEC (Fig. 5B), which was confirmed again by a native PAGE gel (Fig. 5B, inset). The result suggests that the mutation of the two active Cys residues of AtTrx-h3 does not create a pronounced effect on its protein structures and chaperone function. It is a similar result with the previous data showing that the alkylation of active thiols in PDI results in a complete loss of its isomerase activity, but not of the chaperone activity (Quan et al., 1995).

Physiological Significance of AtTrx-h3 in Arabidopsis against Heat Shock

To identify the physiological role of AtTrx-h3 in heat-shock resistance in vivo, we prepared several lines of Arabidopsis T_3 homozygotes, including wild-type Arabidopsis and transgenic Arabidopsis overexpressing empty vector (Vec), AtTrx-h3 (OX), and a T-DNA-inserted knockout line of Arabidopsis (KO1). To demonstrate a functional distinction between the chaperone function of AtTrx-h3 and its disulfide reductase function, we also prepared a transgenic Arabidopsis mutant overexpressing C39/42S (DM) AtTrx-h3, which exhibited only the chaperone function (Fig. 5A). Using 4-week-old seedlings of the various Arabidopsis strains, we analyzed the expression level of AtTrx-h3 by western blotting with an anti-AtTrx-h3 antibody. The immunospecificity of the anti-AtTrx-h3 antibody was verified by both in vivo and in vitro experiments (Supplemental Fig. S5). Although we analyzed the antibody specificity of AtTrx-h3 in vitro by using five AtTrx-h recombinant proteins (h1–h5), Arabidopsis genome contains additional Trx-h isoforms, which differ in part by their sizes and N-terminal extensions (Meyer et al., 2005). Considering the heterologous classification of the proteins in phylogenetic tree (Gelhaye et al., 2004), there may be low probability of other Trx-h isoforms to be recognized by the anti-AtTrx-h3 antibody. Compared with wild-type plants, the transgenic lines strongly overexpressed either the native form of AtTrx-h3 or the C39/42S (DM) mutant, whereas the protein was not expressed in the KO1 line (Fig. 6A, bottom section). Also the oligomeric and HMW complexes in transgenic lines overexpressing the native form of AtTrx-h3 and the C39/42S (DM) mutant protein were significantly higher than that of wild-type Arabidopsis even under the normal conditions estimated by native PAGE (Fig. 6A, top section). During heat shock at 40°C for 3 d and a subsequent recovery period (Fig. 6, B and C, top section), the heat-shock tolerance of the plants was measured. Although

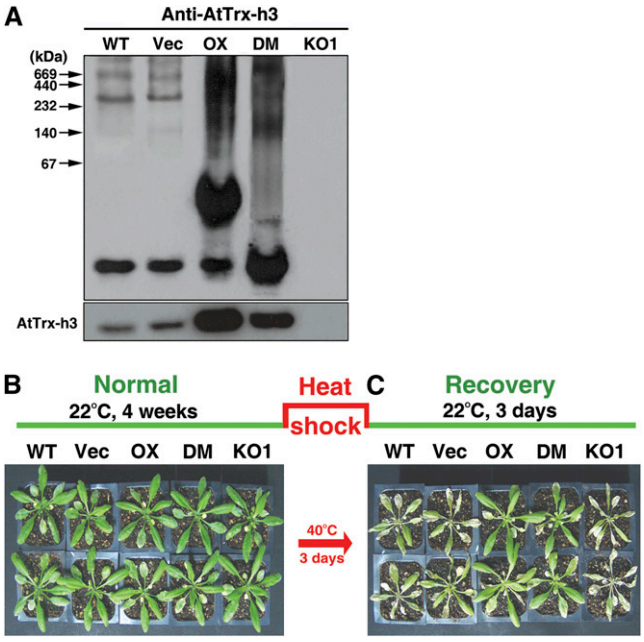

Figure 6. Chaperone function of AtTrx-h3 provides an enhanced heat-shock tolerance for Arabidopsis during the recovery phase after heat shock. A, Expression levels of AtTrx-h3 in wild-type (WT) and transgenic Arabidopsis overexpressing the empty vector (Vec), AtTrx-h3 (OX), C39/42S mutant AtTrx-h3 (DM) proteins, and the T-DNA line of AtTrx-h3-null mutant Arabidopsis (KO1). Cytosolic proteins (50 μg) extracted from 4-week-old Arabidopsis seedlings were subjected to western blotting with an anti-AtTrx-h3 antibody, after separating the proteins on 10% native PAGE (top section) and 12% SDS-PAGE (bottom section) gels. B and C, Comparison of heat-shock tolerance between wild-type and transgenic Arabidopsis seedlings. The process of heat-shock treatment and recovery of the 4-week-old Arabidopsis seedlings is depicted in the top section. B, Before the heat-shock treatment, it was not possible to detect morphological differences between the wild-type and transgenic Arabidopsis plants grown at optimal temperature (22°C) for 4 weeks. C, After heat shock of the plants at 40°C for 3 d, they were transferred to their optimal temperature (22°C) and grown for a further 3 d. Heat-shock tolerance of the wild-type and transgenic Arabidopsis seedlings was compared on the last day of recovery.

4-week-old Arabidopsis plants overexpressing or suppressing AtTrx-h3 showed no phenotypic difference under the optimal growing conditions (Fig. 6B), they significantly suffered from the heat-shock treatment of 40°C for 3 d (data not shown). However, when the heat-treated plants were transferred to their optimal temperature, 22°C, and grown for another 3 d, the transgenic lines overexpressing native AtTrx-h3 or the C39/42S (DM) mutant AtTrx-h3 exhibited enhanced heat-shock tolerance compared with wild-type and control vector plants (Fig. 6C). In contrast, the KO lines demonstrated greater sensitivity to the stress than wild-type plants. The heat-shock-resistant in vivo role of AtTrx-h3 was confirmed again from the plants by measuring the photosynthetic parameters, such as photosynthetic yield and chlorophyll contents. Heat shock caused significant damage in photosynthetic yield and the chlorophyll contents of plants over-

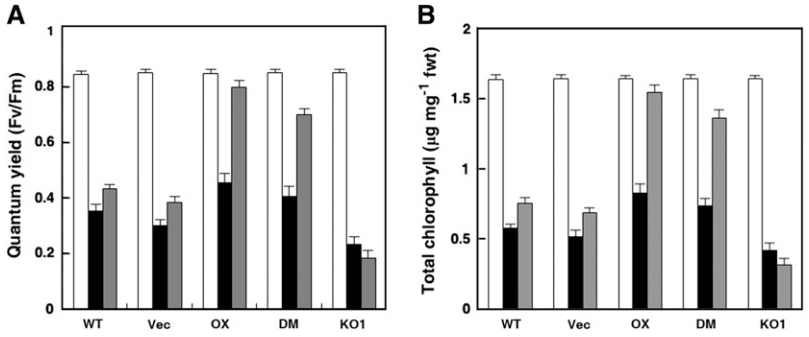

Figure 7. Changes of the photosynthetic parameters of the transgenic Arabidopsis during heat-shock and recovery periods. T_3-homozygote lines of Arabidopsis including wild type (WT), transgenic Arabidopsis overexpressing the empty vector (Vec), AtTrx-h3 (OX), C39/42S mutant AtTrx-h3 (DM), and the T-DNA-inserted knockout (KO1) lines were grown at 22°C for 4 weeks. The plants were heat shocked at 40°C for 3 d and transferred to 22°C (see Fig. 6, B and C, top section). During the heat-shock and recovery periods, changes of the steady-state quantum yield (A) and total chlorophyll contents (B) were compared. The photosynthetic parameters of the 4-week-old Arabidopsis grown at 22°C (white bars) were compared with those of the plants heat shocked at 40°C for 3 d (black bars) and the plants recovered for 3 d at their optimal growing temperature, 22°C (gray bars). fwt, Fresh weight.

expressing or suppressing AtTrx-h3 (Fig. 7). However, whereas the heat-shock-damaged Arabidopsis overexpressing AtTrx-h3 and the C39/42S (DM) protein fully restored the quantum yield and chlorophyll contents during the recovery period, it was not possible for the wild-type and KO lines to recover the parameters. These results suggest that AtTrx-h3 plays a pivotal role in the protection of plant cells from external stresses through its chaperone function.

DISCUSSION

Trx is known to function as a monomer in a variety of cellular reactions (Katti et al., 1990). However, the crystal structure of human Trx revealed that the protein exists as a mixture of functionally active monomers and catalytically inactive homodimers that are stable at slightly acidic conditions (Andersen et al., 1997). In fact, both monomeric and dimeric forms of Trx have been identified in crude extracts of human lymphoid cell lines (Wollman et al., 1988). Despite extensive investigation of the physiological roles played by the Trx dimer, no specific functions have been ascribed to this form. The possible functions of the Trx dimer were presumed to include a mechanism to protect the active sites of proteins during secretion or as part of a regulatory network for sensing oxidative stress in tissues (Weichsel et al., 1996). Also, the interface of the dimer consists primarily of large hydrophobic patches, which provides a potential surface to enable the protein to associate into higher oligomeric complexes. Of potential note are the SEC data of human Trx reported by Andersen et al. (1997), which showed the presence of small amounts of HMW complexes, although they were not investigated in that study.

In this study, we discovered that AtTrx-h3 forms differently sized HMW complexes that correspond closely with its disulfide reductase and chaperone functions, and that the structural and functional switching is regulated by heat shock and redox status. The chaperone function of AtTrx-h3 occurs predominantly in HMW complexes, whereas the disulfide reductase activity occurs in the LMW protein species, which can be summarized by a working model presented in Figure 8. These findings concur with the observations of other cytosolic chaperones, such as 2-Cys Prxs (Chuang et al., 2006; Meissner et al., 2007). In contrast, yeast (*Saccharomyces cerevisiae*) Hsp26 represents the opposite scenario to AtTrx-h3, in that it exists as large oligomeric complexes at 25°C that exhibit a basal level of chaperone activity, whereas upon heat stress they dissociate into dimeric structures that demonstrate greater chaperone activity (Haslbeck et al., 1999). The apparent functions of AtTrx-h3 are regulated by molar ratios of AtTrx-h3 relative to its

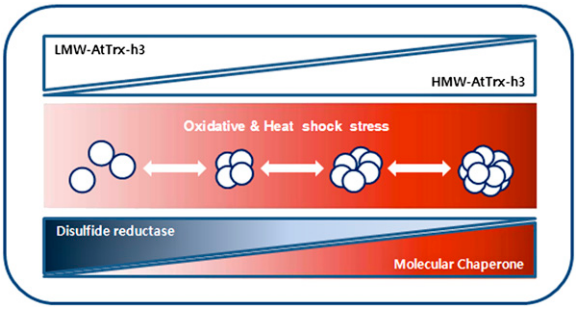

Figure 8. A working model depicting the oxidative stress and heat-shock-dependent structural and functional switching of AtTrx-h3. Under normal conditions, AtTrx-h3 in Arabidopsis predominantly exists as LMW protein species, such as monomers and dimers, and functions as a disulfide reductase. However, when plants are exposed to oxidative and heat stresses, AtTrx-h3 changes its protein structure from LMW to oligomer and HMW complexes, with an accompanying functional switch from a disulfide reductase to a molecular chaperone. [See online article for color version of this figure.]

substrate proteins (Fig. 2). This regulation is similar to that of PDI, which also exhibits concentration-dependent different activities such as antichaperone and chaperone functions (Zhao et al., 2005). However, in contrast to *E. coli* Trx, which is reported to refold partially denatured substrate proteins (Kern et al., 2003), AtTrx-h3 did not exhibit refolding activity of urea-denatured MDH as a substrate (data not shown). On the other hand, it was recently reported that the Trx-h1 efficiently reduced and reactivated the oxidized form of cytosolic MDH in higher plants (Hara et al., 2006). Because the inactivation of important intracellular enzyme by oxidation, such as cytosolic MDH, results in a marked impairment of cell viability, Trx-h1 can act as a redox-sensitive reducer of the protein accompanying its structural transition.

Another major finding in this study is that the AtTrx-h3 protein structure is shifted from LMW to HMW species by redox status and heat shock, concomitantly with functional switching from a disulfide reductase to a molecular chaperone. This may represent a mechanism for protecting the heat-shock-induced nonnative form of substrates from self aggregation, thereby conferring enhanced heat-shock tolerance of plants. Especially, transgenic Arabidopsis plants overexpressing Cys-deficient AtTrx-h3 showed a similar level of heat-shock resistance to those overexpressing the native form of AtTrx-h3, suggesting that heat-shock resistance in plants may be attributed to its chaperone function. This finding is consistent with a report demonstrating that Cys-lacking PDI that retained no isomerase activity improved the viability of a PDI null mutant yeast (LaMantia and Lennarz, 1993).

Our observation that AtTrx-h3 performs dual functions can expand the range of its potential roles in planta, including the maintenance of native conformations of cytosolic proteins against external stresses (Sweat and Wolpert, 2007). A growing body of evidence supports the notion that cytosolic Trxs participate in a variety of cellular processes in higher plants. Recently, it was reported that Trx-mediated conformational changes of NPR1 (for nonexpressor of pathogen-related genes 1) from oligomer to monomer regulated its nuclear localization and gene expression in relation to plant immunity (Tada et al., 2008). Also, from the observation that about 30 rice (*Oryza sativa*) Trx genes showed different temporal and spatial expression patterns and differential responses to phytohormones and light/dark conditions (Nuruzzaman et al., 2008), it was proposed that the individual Trxs appear to perform their unique roles in plants during various aspects of the plant life cycle, such as plant growth, development, and defense responses. In particular, the organ- and developmental stage-specific expression of the eight Trx-h genes in Arabidopsis, AtTrx-hs, also suggests that each isotype of AtTrx-h may have a specific and nonredundant function in plants (Reichheld et al., 2002). This was strongly supported from the finding that AtTrx-h5 is specifically required for victorin sensitivity (Sweat and Wolpert, 2007). In this response, even AtTrx-h3, the Trx most closely related to AtTrx-h5, was not able to compensate for the functional loss of AtTrx-h5. The functional difference between AtTrx-h5 and AtTrx-h3 might be inferred from their expression profiles. Whereas AtTrx-h5 showed a highly inducible expression pattern against various biotic and abiotic stresses, AtTrx-h3 mRNA was constitutively expressed and did not respond to external stresses (Laloi et al., 2004). The results agree well with our data that the expression of AtTrx-h3 at the protein level is not induced by heat shock, but that heat shock regulates its functions by a posttranslational modification.

As chaperones are central components in many signal transduction pathways (Young and Hartl, 2003), identification of the structure-dependent disulfide reductase and chaperone functions of AtTrx-h3 may ultimately enhance our understanding of the as-yet-unidentified cellular functions of cytosolic Trxs in eukaryotic cells.

MATERIALS AND METHODS

Materials

Arabidopsis (*Arabidopsis thaliana*) suspension cells (Arabidopsis L. Heynh., ecotype Columbia) were cultured in Jouanneau and Péaud-Lenoel's medium under continuous white light (100 μmol m^{-2} s^{-1}) with constant shaking (120 rpm) at 22°C, as described (Brault et al., 2004). Arabidopsis plants (ecotype Columbia) were grown under a 16/8 h light/dark cycle at 22°C and 70% humidity. MDH, CS, luciferase, insulin, ovalbumin, and bis-ANS were obtained from Sigma. The HPLC column, model G4000SW_{XL} (7.8 × 300), was from Tosoh. The P-10 desalting column was from GE Healthcare.

Isolation of the HMW Forms of Heat-Stable Proteins from an Arabidopsis Suspension-Cell Culture

To isolate heat-stable proteins having HMW complexes from plant sources, cytosolic extracts were prepared from an Arabidopsis suspension-cell culture, heat treated at 70°C for 30 min, and ultracentrifuged at 134,600*g* for 15 min (Beckman, TLS-55 rotor). The supernatants were subjected to SEC using a TSK G4000SW_{XL} column, and HMW complexes eluting from the void volume of SEC were collected and identified by two-dimensional PAGE and MALDI-TOF analyses, as described (Hajheidari et al., 2007). This procedure enabled us to isolate a heat-stable AtTrx-h3 having HMW protein structures.

Cloning and Mutation of AtTrx-h3 and Expression in *Escherichia coli*

AtTrx-h3 was cloned from an Arabidopsis cDNA library using the PCR, and three proteins containing point mutations (C39S, C42S, and C39/42S) were generated as described (Jang et al., 2004). Recombinant AtTrx-h3 proteins were expressed in *Escherichia coli* BL21 (DE3) using the pGEX expression vector. GST-AtTrx-h3 fusion proteins were purified using a GSH-agarose column, and GST was cleaved by thrombin treatment. After removing other contaminant proteins using an ATP-agarose column, the native form of purified AtTrx-h3 was dialyzed with 50 mM HEPES-KOH (pH 8.0) for use in biochemical analyses and in the preparation of a polyclonal antibody.

Subcellular Localization of AtTrx-h3

The subcellular localization of AtTrx-h3 was analyzed by monitoring the fluorescence of GFP fused to AtTrx-h3 (AtTrx-h3-GFP). AtTrx-h3-GFP DNA was ligated into an expression vector in front of the cauliflower mosaic virus 35S promoter and transformed into Arabidopsis protoplasts obtained from whole seedlings, as described (Abel and Theologis, 1994). Expression of

AtTrx-h3-GFP in transformed protoplasts was examined under a fluorescence microscope (Olympus AX70) with XF116-2 (exciter, 475AF20; dichroic, 500DRLP; emitter, 510AF23) and U-MWU2 filter sets (excitation filter, 330–385; emission filter, 420 nm).

Determination of Disulfide Reductase and Chaperone Activities

Disulfide reductase activity was measured using either DTNB as a substrate in the presence of NADPH and Trx reductase or insulin with DTT as a substrate by absorbance changes at A_{412} and A_{650}, respectively (Dyson et al., 1997). Chaperone activity was measured using MDH, CS, or luciferase as a substrate. The substrate was incubated in 50 mM HEPES-KOH (pH 8.0) buffer at 45°C with various concentrations of AtTrx-h3. After 20 min incubation, thermal aggregation of MDH was determined by monitoring the turbidity increase at A_{650} in a temperature-controlled spectrophotometer (DU800; Beckman), as described (Jang et al., 2004). A SFM25 spectrofluorometer (Kontron) was used to examine bis-ANS binding, which demonstrated exposure of the AtTrx-h3 hydrophobic domain (Sharma et al., 1998).

SEC, PAGE, and Western-Blot Analysis

SEC was performed at 25°C by HPLC (Dionex) using a TSK G4000SW$_{XL}$ column equilibrated with 50 mM HEPES-KOH (pH 8.0) buffer containing 100 mM NaCl, as described (Jang et al., 2004). Reducing and nonreducing SDS-PAGE, or native PAGE as well as western-blot analysis, were performed as described (Moon et al., 2005).

Heat-Shock Resistance of Transgenic Arabidopsis Overexpressing AtTrx-h3

The in vivo role of AtTrx-h3 was investigated using either a T-DNA-inserted knockout line of Arabidopsis (The Arabidopsis Information Resource database: http://www.aspb.org/publications/tairsubmission.cfm) or transgenic Arabidopsis overexpressing the protein. For the construction of transgenic Arabidopsis overexpressing AtTrx-h3, full-length AtTrx-h3 cDNA was ligated into the binary vector pCAMBIA1300 and transformed into plants (Clough and Bent, 1998). Transgenic expression was observed using reverse transcription-PCR and western-blot analyses. For the heat-shock resistance experiment, wild-type and T_3 lines of transgenic Arabidopsis were grown for 4 weeks at their optimal growing temperature (22°C), heat treated at 40°C for 3 d, and then returned to 22°C. The recovery capacity of the plants following heat shock was then analyzed. All the data presented are averages of at least three independent measurements.

Measurement of Photosynthetic Parameters

For the measurement of Arabidopsis thermotolerance, chlorophyll content and chlorophyll fluorescence were analyzed. The chlorophyll quantity extracted using 80% (v/v) acetone was measured as described (Porra et al., 1989), and the chlorophyll fluorescence (quantum yield of PSII, F_v/F_m) was analyzed with a portable fluorometer (Handy PEA; Hansatech) as described (Shahbazi et al., 2007). At least three leaves from each Arabidopsis plant were examined for the estimation of the F_v/F_m ratio.

Sequence data from this article can be found in the GenBank/EMBL data libraries under accession number At5g42980.

Supplemental Data

The following materials are available in the online version of this article.

Supplemental Figure S1. Verification of protein purity and identification of AtTrx-h3 by MALDI-TOF analysis.

Supplemental Figure S2. Chaperone activity of AtTrx-h3 measured by using the CS or luciferase as substrates.

Supplemental Figure S3. Rechromatography of the three AtTrx-h3 fractions separated by SEC (F-I to F-III).

Supplemental Figure S4. Redox-dependent structural changes of AtTrx-h3 in SEC.

Supplemental Figure S5. Immunospecificity of the anti-AtTrx-h3 antibody.

Received January 8, 2009; accepted March 26, 2009; published April 1, 2009.

LITERATURE CITED

Abel S, Theologis A (1994) Transient transformation of Arabidopsis leaf protoplasts: a versatile experimental system to study gene expression. Plant J **5:** 421–427

Andersen JF, Sanders DA, Gasdaska JR, Weichsel A, Powis G, Montfort WR (1997) Human thioredoxin homodimers: regulation by pH, role of aspartate 60, and crystal structure of the aspartate 60 → asparagine mutant. Biochemistry **36:** 13979–13988

Aslund F, Beckwith J (1999) Bridge over troubled waters: sensing stress by disulfide bond formation. Cell **96:** 751–753

Balmer Y, Koller A, del Val G, Manieri W, Schurmann P, Buchanan BB (2003) Proteomics gives insight into the regulatory function of chloroplast thioredoxins. Proc Natl Acad Sci USA **100:** 370–375

Brault M, Amiar Z, Pennarun AM, Monestiez M, Zhang Z, Cornel D, Dellis O, Knight H, Bouteau F, Rona JP (2004) Plasma membrane depolarization induced by abscisic acid in Arabidopsis suspension cells involves reduction of proton pumping in addition to anion channel activation, which are both Ca^{2+} dependent. Plant Physiol **135:** 231–243

Chuang MH, Wu MS, Lo WL, Lin JT, Wong CH, Chiou SH (2006) The antioxidant protein alkylhydroperoxide reductase of Helicobacter pylori switches from a peroxide reductase to a molecular chaperone function. Proc Natl Acad Sci USA **103:** 2552–2557

Clough SJ, Bent AF (1998) Floral dip: a simplified method for Agrobacterium-mediated transformation of Arabidopsis thaliana. Plant J **16:** 735–743

Datta SA, Rao CM (1999) Differential temperature-dependent chaperone-like activity of alphaA- and alphaB-crystallin homoaggregates. J Biol Chem **274:** 34773–34778

Davidson JF, Whyte B, Bissinger PH, Schiestl RH (1996) Oxidative stress is involved in heat-induced cell death in Saccharomyces cerevisiae. Proc Natl Acad Sci USA **93:** 5116–5121

Dyson HJ, Jeng MF, Tennant LL, Slaby I, Lindell M, Cui DS, Kuprin S, Holmgren A (1997) Effects of buried charged groups on cysteine thiol ionization and reactivity in Escherichia coli thioredoxin: structural and functional characterization of mutants of Asp 26 and Lys 57. Biochemistry **36:** 2622–2636

Feng JN, Russel M, Model P (1997) A permeabilized cell system that assembles filamentous bacteriophage. Proc Natl Acad Sci USA **94:** 4068–4073

Gelhaye E, Rouhier N, Jacquot JP (2004) The thioredoxin h system of higher plants. Plant Physiol Biochem **42:** 265–271

Hajheidari M, Eivazi A, Buchanan BB, Wong JH, Majidi I, Salekdeh GH (2007) Proteomics uncovers a role for redox in drought tolerance in wheat. J Proteome Res **6:** 1451–1460

Haley DA, Horwitz J, Stewart PL (1998) The small heat-shock protein, alphaB-crystallin, has a variable quaternary structure. J Mol Biol **277:** 27–35

Hamdan SM, Marintcheva B, Cook T, Lee SJ, Tabor S, Richardson CC (2005) A unique loop in T7 DNA polymerase mediates the binding of helicase-primase, DNA binding protein, and processivity factor. Proc Natl Acad Sci USA **102:** 5096–5101

Hara S, Motohashi K, Arisaka F, Romano PG, Hosoya-Matsuda N, Kikuchi N, Fusada N, Hisabori T (2006) Thioredoxin-h1 reduces and reactivates the oxidized cytosolic malate dehydrogenase dimer in higher plants. J Biol Chem **281:** 32065–32071

Haslbeck M, Walke S, Stromer T, Ehrnsperger M, White HE, Chen S, Saibil HR, Buchner J (1999) Hsp26: a temperature-regulated chaperone. EMBO J **18:** 6744–6751

Holmgren A, Bjornstedt M (1995) Thioredoxin and thioredoxin reductase. Methods Enzymol **252:** 199–208

Ishiwatari Y, Honda C, Kawashima I, Nakamura S, Hirano H, Mori S, Fujiwara T, Hayashi H, Chino M (1995) Thioredoxin h is one of the major proteins in rice phloem sap. Planta **195:** 456–463

Jang HH, Lee KO, Chi YH, Jung BG, Park SK, Park JH, Lee JR, Lee SS, Moon JC, Yun JW, et al (2004) Two enzymes in one; two yeast

peroxiredoxins display oxidative stress-dependent switching from a peroxidase to a molecular chaperone function. Cell **117:** 625–635

Katti SK, LeMaster DM, Eklund H (1990) Crystal structure of thioredoxin from Escherichia coli at 1.68 A resolution. J Mol Biol **212:** 167–184

Kern R, Malki A, Holmgren A, Richarme G (2003) Chaperone properties of *Escherichia coli* thioredoxin and thioredoxin reductase. Biochem J **371:** 965–972

Laloi C, Mestres-Ortega D, Marco Y, Meyer Y, Reichheld JP (2004) The Arabidopsis cytosolic thioredoxin h5 gene induction by oxidative stress and its W-box-mediated response to pathogen elicitor. Plant Physiol **134:** 1006–1016

Laloi C, Rayapuram N, Chartier Y, Grienenberger JM, Bonnard G, Meyer Y (2001) Identification and characterization of a mitochondrial thioredoxin system in plants. Proc Natl Acad Sci USA **98:** 14144–14149

LaMantia ML, Lennarz WJ (1993) The essential function of yeast protein disulfide isomerase does not reside in its isomerase activity. Cell **74:** 899–908

Marchand C, Le Marechal P, Meyer Y, Miginiac-Maslow M, Issakidis-Bourguet E, Decottignies P (2004) New targets of Arabidopsis thioredoxins revealed by proteomic analysis. Proteomics **4:** 2696–2706

Marcus F, Chamberlain SH, Chu C, Masiarz FR, Shin S, Yee BC, Buchanan BB (1991) Plant thioredoxin h: an animal-like thioredoxin occurring in multiple cell compartments. Arch Biochem Biophys **287:** 195–198

Meissner U, Schröder E, Scheffler D, Martin AG, Harris JR (2007) Formation, TEM study and 3D reconstruction of the human erythrocyte peroxiredoxin-2 dodecahedral higher-order assembly. Micron **38:** 29–39

Meyer Y, Reichheld JP, Vignols F (2005) Thioredoxins in Arabidopsis and other plants. Photosynth Res **86:** 419–433

Moon JC, Hah YS, Kim WY, Jung BG, Jang HH, Lee JR, Kim SY, Lee YM, Jeon MG, Kim CW, et al (2005) Oxidative stress-dependent structural and functional switching of a human 2-Cys peroxiredoxin isotype II that enhances HeLa cell resistance to H_2O_2-induced cell death. J Biol Chem **280:** 28775–28784

Nuruzzaman M, Gupta M, Zhang C, Wang L, Xie W, Xiong L, Zhang Q, Lian X (2008) Sequence and expression analysis of the thioredoxin protein gene family in rice. Mol Genet Genomics **280:** 139–151

Porra RJ, Thompson WA, Kriedemann PE (1989) Determination of accurate extinction coefficients and simultaneous equations for assaying chlorophyll a and b extracted with four different solvents: verification of the concentration of chlorophyll standards by atomic absorption spectroscopy. Biochim Biophys Acta **975:** 384–394

Quan H, Fan G, Wang CC (1995) Independence of the chaperone activity of protein disulfide isomerase from its thioredoxin-like active site. J Biol Chem **270:** 17078–17080

Ravi D, Muniyappa H, Das KC (2005) Endogenous thioredoxin is required for redox cycling of anthracyclines and p53-dependent apoptosis in cancer cells. J Biol Chem **280:** 40084–40096

Reichheld JP, Mestres-Ortega D, Laloi C, Meyer Y (2002) The multigenic family of thioredoxin h in *Arabidopsis thaliana*: specific expression and stress response. Plant Physiol Biochem **40:** 685–690

Serrato AJ, Cejudo FJ (2003) Type-h thioredoxins accumulate in the nucleus of developing wheat seed tissues suffering oxidative stress. Planta **217:** 392–399

Shahbazi M, Gilbert M, Labouré AM, Kuntz M (2007) Dual role of the plastid terminal oxidase in tomato. Plant Physiol **145:** 691–702

Sharma KK, Kaur H, Kumar GS, Kester K (1998) Interaction of 1,1′-bi(4-anilino)naphthalene-5,5′-disulfonic acid with alpha-crystallin. J Biol Chem **273:** 8965–8970

Sweat TA, Wolpert TJ (2007) Thioredoxin h5 is required for victorin sensitivity mediated by a CC-NBS-LRR gene in *Arabidopsis*. Plant Cell **19:** 673–687

Tada Y, Spoel SH, Pajerowska-Mukhtar K, Mou Z, Song J, Wang C, Zuo J, Dong X (2008) Plant immunity requires conformational charges of NPR1 via S-nitrosylation and thioredoxins. Science **321:** 952–956

The Arabidopsis Genome Initiative (2000) Analysis of the genome sequence of the flowering plant *Arabidopsis thaliana*. Nature **408:** 796–815

Weichsel A, Gasdaska JR, Powis G, Montfort WR (1996) Crystal structures of reduced, oxidized, and mutated human thioredoxins: evidence for a regulatory homodimer. Structure **4:** 735–751

Wollman EE, d'Auriol L, Rimsky L, Shaw A, Jacquot JP, Wingfield P, Graber P, Dessarps F, Robin P, Galibert F, et al (1988) Cloning and expression of a cDNA for human thioredoxin. J Biol Chem **263:** 15506–15512

Wolosiuk RA, Ballicora MA, Hagelin K (1993) The reductive pentose phosphate cycle for photosynthetic CO_2 assimilation: enzyme modulation. FASEB J **7:** 622–637

Young JC, Hartl FU (2003) A stress sensor for the bacterial periplasm. Cell **113:** 1–2

Zhao TJ, Ou WB, Xie Q, Liu Y, Yan YB, Zhou HM (2005) Catalysis of creatine kinase refolding by protein disulfide isomerase involves disulfide cross-link and dimer to tetramer switch. J Biol Chem **280:** 13470–13476